

Shape optimization using Weibull statistics of brittle failure

E. Lund

Institute of Mechanical Engineering, Aalborg University, DK-9220 Aalborg, Denmark

Abstract This paper is devoted to the problem of designing mechanical components of brittle materials such as ceramics using the Weibull probabilistic treatment of brittle strength combined with finite element based design optimization and mathematical programming. The analysis of probability of failure using Weibull statistics is introduced and expressions for design sensitivity analysis are derived. The numerical finite element based implementation is discussed, and a numerical example is used to verify the facilities for analysis and design sensitivity analysis. Finally, a shape optimization example of redesigning a cutting bit from a circular saw blade illustrates a design case where the objective is to reduce the probability of failure.

1 Introduction

Design optimization problems involving Weibull statistics are rarely discussed but design with brittle materials such as ceramics calls for use of structural shape optimization as design with new materials very often cannot be based on design rules or engineering tradition. One of the few examples of using structural shape optimization in the design of ceramic components can be found in a very interesting paper by Koski and Silvenninen (1990).

In the last decades there has been an increasing use of ceramic materials in mechanical engineering applications where good wear resistance properties, high hardness, sufficient high-temperature capability, high stiffness, and good corrosion resistance are needed. However, design with ceramic materials is different from design with traditional ductile materials due to the brittle behaviour of ceramics.

The use of brittle materials for load carrying components involves two basic features that must be taken into account in the design phase. First, the material has very low strain tolerance and practically exhibits no yielding. Thus, the material behaviour is linearly elastic up to the fracture point where an unstable crack growth suddenly takes place. Second, there is frequently large scatter in the strength data so probabilistic methods must be used.

A reliability evaluation based on a two-parameter Weibull distribution has been generally accepted in design of brittle materials (see e.g. McLean and Hartsock 1989), and this probabilistic treatment of the brittle strength will be used throughout this paper. Weibull (1939) developed a probabilistic failure criterion based only on tensile stresses in the component. Compressive failure is not considered in this criterion because brittle materials usually fail from tensile stresses due to their very high compressive strength.

2 Analysis of probability of failure

The probability of failure for a component made of a brittle material can be computed from its stress field by using the weakest link theory based on the Weibull distribution, and for uniaxial stress, Weibull established the following function that describes the cumulative probability of failure P_f of a ceramic component

$$P_f = 1 - \exp \left[- \left(\frac{1}{m} \right)^m \frac{1}{V_c} \int_V \left(\frac{\sigma}{\sigma_c} \right)^m dV \right], \quad (1)$$

where σ is the tensile stress at a given point, m the Weibull modulus, and σ_c the characteristic mean fracture stress associated with a characteristic reference volume V_c ; V is the total volume of the component and the term

$$\left(\frac{1}{m} \right)^m = \Gamma \left(\frac{1}{m} + 1 \right) = \int_0^{\infty} t^{\frac{1}{m}} \exp[-t] dt \quad (2)$$

is the value of the gamma function Γ at $\frac{1}{m} + 1$ which is easily evaluated.

Equation (1) indicates that in order to obtain an optimum design with respect to strength of a component made of a brittle material, it is usually not sufficient just to minimize the larger principal stresses in the structure. It is necessary to take into account the amount of material subjected to the largest tensile stresses, as a larger volume has a larger probability of containing big flaws than a smaller volume of the structure.

In order to generalize (1) to three-dimensional stress states, the concept of integrating the normal stress σ_n and the maximum shear stress τ around the portion of the unit radius sphere where the normal stress is positive is generally used (see e.g. Vardar and Finnie 1975; Evans 1978; McLean and Hartsock 1989; Andreasen 1993, 1994; and Fig. 1).

The normal stress σ_n and the maximum shear stress τ acting on a single crack are defined as

$$\sigma_n = \mathbf{n} \cdot \boldsymbol{\sigma} \cdot \mathbf{n}, \quad \tau^2 = \mathbf{n} \cdot \boldsymbol{\sigma}^2 \cdot \mathbf{n} - \sigma_n^2, \quad (3)$$

with $\boldsymbol{\sigma}$ as the stress tensor and \mathbf{n} as the normal vector to the unit sphere. Then, at a given location on the unit sphere these stresses are given as

$$\sigma_n = \cos^2 \phi \left(\sigma_1 \cos^2 \psi + \sigma_2 \sin^2 \psi \right) + \sigma_3 \sin^2 \phi,$$

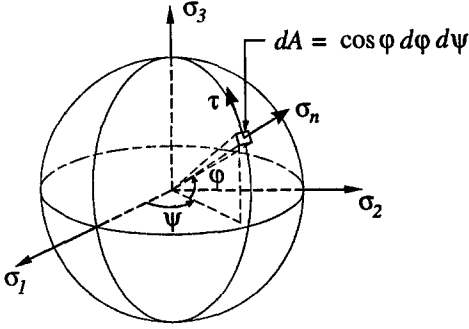


Fig. 1. Geometric variables describing location on the unit sphere

$$\tau = \sqrt{\cos^2 \phi (\sigma_1^2 \cos^2 \psi + \sigma_2^2 \sin^2 \psi) + \sigma_3^2 \sin^2 \phi - \sigma_n^2}. \quad (4)$$

An equivalent stress σ_e that is a function of σ_n and τ is introduced, i.e. $\sigma_e = \sigma_e(\sigma_n, \tau)$. The combination of stresses causing failure is not uniquely determined due to a lack of knowledge of the precise geometry of the actual flaws in the structure and a lack of consensus regarding an appropriate crack extension criterion as stated by Andreassen (1993). Therefore, different definitions of the equivalent stress can be chosen, depending on the wanted influence of shear stresses in the fracture criterion. Four different criteria that are used to define the equivalent stress σ_e can be found in Table 1.

The normal stress averaging criterion pertains to non-shear sensitive cracks and is also termed "mode I failure criterion". The maximum strain release rate criterion is obtained from two-dimensional Griffith cracks, the third criterion is obtained from non-coplanar crack growth of Griffith cracks, and the last criterion assumes that there is no interaction between the principal stresses $\sigma_k, k = 1, \dots, 3$, in the fracture criterion, i.e. the integration over the unit sphere is omitted.

Thus, integrating this equivalent stress σ_e over the unit sphere with area A_{us} , the general equation for the probability of failure for a three-dimensional stress state is

$$P_f = 1 - \exp[-B], \quad (5)$$

where the exponent B , known as the risk of rupture, is given as

$$B = \left(\frac{1}{m}\right)^m \frac{1}{V_c} \int_V \left[k \int_{A_{us}} \left(\frac{\sigma_e}{\sigma_c}\right)^m dA \right] dV. \quad (6)$$

The factor k is a compatibility term to force the equation to reduce to the original equation for uniaxial tension, see (1). If one of the first three definitions of the equivalent stress in Table 1 is used, the compatibility term k in (6) is given as $k = (2m + 1)/(2\pi)$. If the principle of independent action of the principal stresses is assumed, the integration over the unit sphere is omitted and the compatibility term $k = 1$.

Having defined the equivalent stress σ_e , the risk of rupture B in (6) and thereby the probability of failure in (5) can be evaluated based on a given stress field.

3 Design sensitivity analysis

Next the necessary expressions for design sensitivity analysis of the probability of failure will be derived. The design variables can be shape, sizing or material design variables and will be denoted by $a_i, i = 1, \dots, I$. Differentiating the probability of failure P_f given by (5) with respect to a design variable a_i , the derivative is found as

$$\frac{\partial P_f}{\partial a_i} = \exp[-B] \frac{\partial B}{\partial a_i}, \quad i = 1, \dots, I. \quad (7)$$

The derivative of the risk of rupture $B = B(\sigma_1, \sigma_2, \sigma_3, V)$ can be found by applying the chain rule

$$\frac{\partial B}{\partial a_i} = \sum_{k=1}^3 \frac{\partial B}{\partial \sigma_k} \frac{\partial \sigma_k}{\partial a_i} + \frac{\partial B}{\partial V} \frac{\partial V}{\partial a_i}, \quad (8)$$

where $\sigma_k, k = 1, 2, 3$, are the principal stresses. The terms involved in (8) are derived in the following.

As B is defined in terms of the equivalent stress $\sigma_e = \sigma_e(\sigma_n, \tau)$ the chain rule is applied on the derivative $\partial B / \partial \sigma_k, k = 1, 2, 3$

$$\frac{\partial B}{\partial \sigma_k} = \frac{\partial B}{\partial \sigma_n} \frac{\partial \sigma_n}{\partial \sigma_k} + \frac{\partial B}{\partial \tau} \frac{\partial \tau}{\partial \sigma_k}. \quad (9)$$

The derivative $\partial B / \partial \sigma_n$ is given as

$$\frac{\partial B}{\partial \sigma_n} = \left(\frac{1}{m}\right)^m \frac{1}{V_c} \int_V \left[k \int_{A_{us}} \frac{\partial \left(\frac{\sigma_e}{\sigma_c}\right)^m}{\partial \sigma_n} dA \right] dV, \quad (10)$$

and the derivative $\partial B / \partial \tau$ is found in a similar way.

The derivatives $\partial \sigma_e^m / \partial \sigma_n$ in (10) and $\partial \sigma_e^m / \partial \tau$ depend on the definition of the equivalent stress σ_e and can be seen in Table 2.

Please note that in case of the principle of independent action criterion the partial derivatives $\partial \sigma_e^m / \partial \sigma_k, k = 1, 2, 3$, and thereby the derivative $\partial B / \partial \sigma_k$ to be inserted in (8), are found directly.

The derivatives of the normal stress σ_n and the maximum shear stress τ with respect to the principal stresses $\sigma_k, k = 1, 2, 3$, to be inserted in (9) are easily derived as

$$\begin{aligned} \frac{\partial \sigma_n}{\partial \sigma_1} &= \cos^2 \phi \cos^2 \psi, & \frac{\partial \sigma_n}{\partial \sigma_2} &= \cos^2 \phi \sin^2 \psi, \\ \frac{\partial \sigma_n}{\partial \sigma_3} &= \sin^2 \phi, \end{aligned} \quad (11)$$

and

$$\begin{aligned} \frac{\partial \tau}{\partial \sigma_1} &= \frac{\cos^2 \phi \cos^2 \psi (\sigma_1 - \sigma_n)}{\tau}, \\ \frac{\partial \tau}{\partial \sigma_2} &= \frac{\cos^2 \phi \sin^2 \psi (\sigma_2 - \sigma_n)}{\tau}, \\ \frac{\partial \tau}{\partial \sigma_3} &= \frac{\sin^2 \phi (\sigma_3 - \sigma_n)}{\tau}. \end{aligned} \quad (12)$$

The sensitivities of the principal stresses, $\partial \sigma_k / \partial a_i$, needed in (8), are computed by a standard design sensitivity

Table 1. Different definitions of the equivalent stress σ_e

Name of equivalent stress criterion	Definition
Normal stress averaging criterion	$\sigma_e = \begin{cases} \sigma_n & \text{if } \sigma_n > 0 \\ 0 & \text{if } \sigma_n \leq 0 \end{cases}$
Maximum strain release rate criterion	$\sigma_e = \begin{cases} \sqrt{\sigma_n^2 + \tau^2} & \text{if } \sigma_n > 0 \\ 0 & \text{if } \sigma_n \leq 0 \end{cases}$
Max. noncoplanar strain release rate crit.	$\sigma_e = \begin{cases} \sqrt[4]{\sigma_n^4 + 6\sigma_n^2\tau^2 + \tau^4} & \text{if } \sigma_n > 0 \\ 0 & \text{if } \sigma_n \leq 0 \end{cases}$
Principle of independent action criterion	$\sigma_e = \sum_{k=1}^3 \langle \sigma_k \rangle$ where $\langle \sigma_k \rangle = \begin{cases} \sigma_k & \text{if } \sigma_k > 0 \\ 0 & \text{if } \sigma_k \leq 0 \end{cases}$

Table 2. Derivative of the equivalent stress σ_e (definitions given in Table 1)

Name of equivalent stress criterion	Derivative
Normal stress averaging criterion	$\frac{\partial \sigma_e^m}{\partial \sigma_n} = m \sigma_e^{m-1}, \quad \frac{\partial \sigma_e^m}{\partial \tau} = 0$
Maximum strain release rate criterion	$\frac{\partial \sigma_e^m}{\partial \sigma_n} = m \sigma_n \sigma_e^{m-2}, \quad \frac{\partial \sigma_e^m}{\partial \tau} = m \tau \sigma_e^{m-2}$
Max. noncoplanar strain release rate crit.	$\frac{\partial \sigma_e^m}{\partial \sigma_n} = m (\sigma_n^3 + 3\sigma_n \tau^2) \sigma_e^{m-4},$ $\frac{\partial \sigma_e^m}{\partial \tau} = m (\tau^3 + 3\sigma_n^2 \tau) \sigma_e^{m-4}$
Principle of independent action criterion	$\frac{\partial \sigma_e^m}{\partial \sigma_k} = m \langle \sigma_k \rangle^{m-1}, \quad k = 1, 2, 3$

analysis (see e.g. Lund 1994). If the analysis is finite element based and the analysis considered is static with possible thermal effects included, the equilibrium equation is given as

$$\mathbf{K}\mathbf{D} = \mathbf{F}, \quad (13)$$

where \mathbf{K} is the global stiffness matrix, \mathbf{F} the global consistent load vector and \mathbf{D} the global displacement vector. Using the direct differentiation approach, the displacement sensitivities can be computed efficiently from

$$\mathbf{K}(\mathbf{a}) \frac{\partial \mathbf{D}}{\partial a_i} = -\frac{\partial \mathbf{K}(\mathbf{a})}{\partial a_i} \mathbf{D} + \frac{\partial \mathbf{F}}{\partial a_i}, \quad i = 1, \dots, I, \quad (14)$$

where the factorized stiffness matrix \mathbf{K} can be reused, i.e. a forward-backward substitution with the new right-hand side, the so-called pseudo load vector, yields the displacement sensitivities. The derivative $\partial \mathbf{K} / \partial a_i$ is computed at the element

level, and analytical sensitivities are used in the case of thickness or material design variables. In the case of shape design variables, the method of "exact" semianalytical sensitivity analysis is used (see Olhoff *et al* 1993; Lund and Olhoff 1994; Lund 1994).

At the element level, the stresses are computed from

$$\boldsymbol{\sigma} = \mathbf{E} (\boldsymbol{\varepsilon} - \boldsymbol{\varepsilon}^{\text{th}}) = \mathbf{E} (\mathbf{B}\mathbf{d} - \boldsymbol{\varepsilon}^{\text{th}}), \quad (15)$$

where \mathbf{E} is the constitutive matrix, $\boldsymbol{\varepsilon}$ the strain vector, $\boldsymbol{\varepsilon}^{\text{th}}$ the thermally induced strains, \mathbf{B} the element strain-displacement matrix and \mathbf{d} the element displacement vector. The stress sensitivities can be obtained directly as

$$\frac{\partial \boldsymbol{\sigma}}{\partial a_i} = \mathbf{E} \left(\frac{\partial \mathbf{B}}{\partial a_i} \mathbf{d} + \mathbf{B} \frac{\partial \mathbf{d}}{\partial a_i} - \frac{\partial \boldsymbol{\varepsilon}^{\text{th}}}{\partial a_i} \right), \quad (16)$$

where the sensitivities of the thermally induced strains are given as

$$\frac{\partial \epsilon^{\text{th}}}{\partial a_i} = \left\{ \frac{\partial T}{\partial a_i} \frac{\partial T}{\partial a_i} \frac{\partial T}{\partial a_i} 0 0 0 \right\}^T \alpha. \quad (17)$$

Here α is a matrix containing thermal expansion coefficients and the temperature sensitivities $\partial T/\partial a_i$ are obtained from a thermal design sensitivity analysis derived in a similar way as (14). The sensitivities of the principal stresses, $\partial \sigma_k/\partial a_i$, are obtained directly from the stress sensitivities given by (16).

Table 3. Computed sensitivities of probability of failure for the test specimen example

Relative perturbation	Absolute perturbation	Finite difference	Analytical evaluation
$\frac{\Delta a_1}{\text{height}}$	Δa_1	$\frac{\Delta P_f}{\Delta a_1}$	$\frac{\partial P_f}{\partial a_1}$
10^{-1}	1.0	$2.838 \cdot 10^{-2}$	$3.724 \cdot 10^{-2}$
10^{-2}	10^{-1}	$3.616 \cdot 10^{-2}$	$3.724 \cdot 10^{-2}$
10^{-3}	10^{-2}	$3.713 \cdot 10^{-2}$	$3.724 \cdot 10^{-2}$
10^{-4}	10^{-3}	$3.723 \cdot 10^{-2}$	$3.724 \cdot 10^{-2}$
10^{-5}	10^{-4}	$3.724 \cdot 10^{-2}$	$3.724 \cdot 10^{-2}$
10^{-6}	10^{-5}	$3.724 \cdot 10^{-2}$	$3.724 \cdot 10^{-2}$
10^{-7}	10^{-6}	$3.724 \cdot 10^{-2}$	$3.724 \cdot 10^{-2}$

Finally, the volume sensitivity $\partial V/\partial a_i$ used in (8) is computed from geometric information and the derivative of B with respect to the volume V is given as

$$\frac{\partial B}{\partial V} = \left(\frac{1}{m!} \right)^m \frac{1}{V_c} \left[k \int_{A_{us}} \left(\frac{\sigma_e}{\sigma_c} \right)^m dA \right]. \quad (18)$$

Now all terms needed for computing the derivative of the probability of failure, see (7) and (8), have been determined.

4 Numerical implementation

Numerical facilities for evaluating these expressions for analysis and design sensitivity analysis of the probability of failure of a mechanical component have been implemented in the general purpose design optimization system ODESSY which are being developed at the Institute of Mechanical Engineering, Aalborg University (see Rasmussen *et al.* 1993; Lund 1994). This system contains facilities for a very general geometric description of the design optimization model and is integrated with the two commercial CAD systems AutoCAD and Pro/ENGINEER. The analysis facilities in the system are finite element based and these modules have been used for computing the stress field which is the basis for evaluating the probability of failure.

However, the computation of B in (5) involves several difficulties which will be discussed in the following. The evaluation of B is based on the following expression, see (6):

$$B = \left(\frac{1}{m!} \right)^m \frac{1}{V_c} \sum_{i=1}^{n_e} \int_{V_e} \left[k \int_{A_{us}} \left(\frac{\sigma_e}{\sigma_c} \right)^m dA \right] dV_e. \quad (19)$$

Gauss quadrature

The volume integral is carried out using Gauss quadrature, and the number of integration points used for each finite element depends on the Weibull modulus m . That is, the stress field first is computed in each finite element at the traditional superconvergent positions and these values are then used to compute the stresses at any integration point in the evaluation of B . For a Weibull modulus m the Gauss integration must be of order $(m+1)/2$ in order to evaluate the volume integral accurately.

At each volume integration point another integration over the unit sphere must be carried out and this area integral is in the current implementation also computed using Gauss quadrature. Other integration schemes might be more efficient but have not yet been implemented. The evaluation of the probability of failure thereby involves large computational efforts.

Finally, it should be noted that in order to obtain reliable results for the probability of failure the larger stresses in the structure must be computed accurately and this may require a finite element model with many degrees of freedom. The computational time involved in computing the probability of failure depends almost linearly on the number of finite elements used and it is therefore an advantage to use a coarse mesh consisting of higher order finite elements. This fact should be taken into account when creating the finite element analysis model.

5 Numerical test example

The numerical facilities for computing the probability of failure have been implemented for a number of 2D and 3D isoparametric solid finite elements and comparisons with analytical solutions have been used to verify the implementation. A simple test example is shown in Fig. 2.

The test specimen in Fig. 2 has unit thickness and dimension 50×10 mm. It is subjected to uniform tensile stresses of size 600 MPa, and the material has a characteristic mean fracture stress σ_c of 1000 MPa associated with a reference volume V_c of 10 mm^3 and Weibull modulus m of 10. Based on (1), the probability of failure can be computed analytically to 0.1678, i.e. 16.78%. The finite element model consists of 45 eight-node isoparametric 2D solid finite elements, and the numerical result agrees within numerical accuracy with the analytical result.

Next the analytical expressions for design sensitivity analysis are verified by comparing with finite difference results. The upper boundary of the test specimen is modelled by a

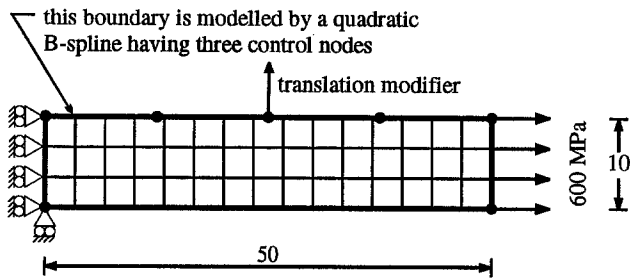


Fig. 2. Design model of test specimen

quadratic B-spline having three control nodes, and the vertical translation of the middle control node is used as shape design variable a_1 . Different translation sizes are used to compare the results obtained using forward finite difference sensitivity evaluations and the analytical expressions derived in this paper. The method of "exact" semianalytical sensitivity analysis is used to determine the stress sensitivities when computing the analytical expressions. The results can be seen in Table 3.

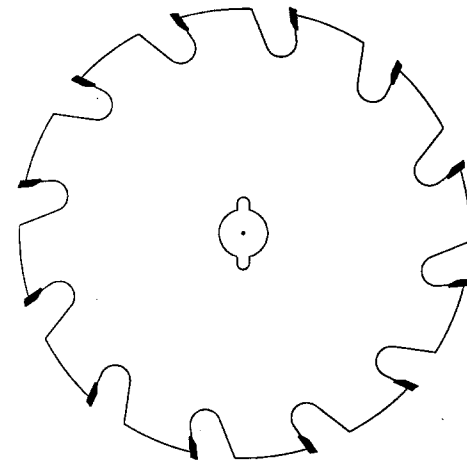
The finite difference evaluations of the sensitivity of probability of failure verify the analytical expressions as seen in Table 3, and the step size problem involved in using finite difference evaluations is completely removed by using the analytical expressions for design sensitivity analysis. The design sensitivity analysis has been verified by comparisons with finite difference evaluations for many other examples and agreement between the two methods have been obtained in all examples.

6 Shape optimization of cutting bit from a circular saw blade

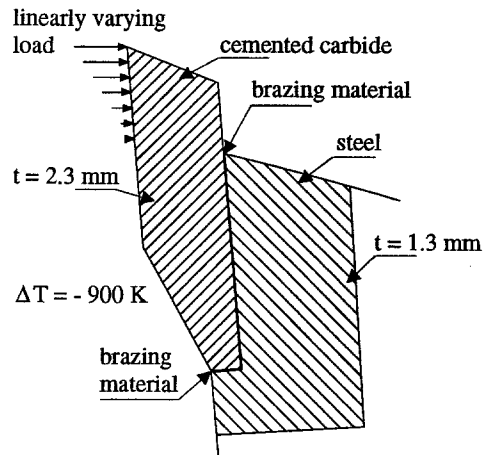
An example of minimizing the probability of failure of a mechanical component made of a brittle material is given in this section. The example deals with shape optimization of a cutting bit from a circular saw blade as illustrated in Fig. 3.

The saw blade is made of steel and the cutting bit of a cemented carbide. The cutting bit is brazed to the saw blade at a temperature of approximately 920°C and the structure is then cooled down. This process causes thermally induced stresses which are taken into account. Furthermore, a linearly varying load corresponding to the maximum loading situation is applied at the cutting bit. This maximum mechanical loading has very little influence on the resulting stress field which is primarily governed by the eigenstress field from the brazing process. The cemented carbide has a characteristic mean fracture stress σ_c of 1300 MPa associated with a reference volume V_c of 13 mm^3 and Weibull modulus m of 11.

A 2D finite element model is used and the objective is to redesign the shape of the cutting bit such that the probability of failure in this maximum loading situation is minimized. The only constraints originate in allowable geometric changes of the shape of the cutting bit, i.e. the volume of the cutting bit is allowed to increase from the initial design. Constraints on shear stresses at the interface between the cutting bit and the saw blade could be considered in the optimization problem but are excluded in this example. The optimization



circular saw blade ($D = 150 \text{ mm}$)



zoom on cutting bit

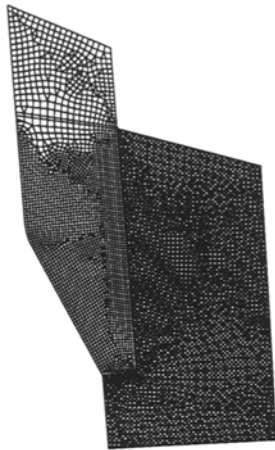
Fig. 3. Circular saw blade ($D = 150 \text{ mm}$)

problem thus can be stated as

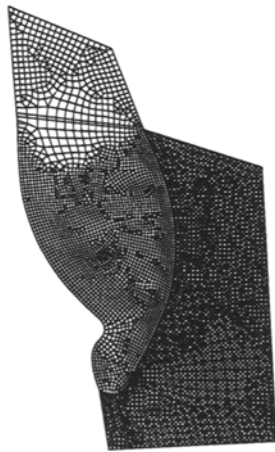
minimize the probability of failure of the cutting bit.

The boundaries are described by quadratic B-splines having 19 shape design variables and a SLP algorithm is used as optimizer. The finite element model consists of approximately 5000 quadratic 2D solid finite elements. The probability of failure of the initial design is $P_f = 4.7\%$, i.e. 1 out of 21 bits fails but having performed the shape optimization the probability of failure is reduced to $P_f = 0.0014\%$, i.e. 1 out of 7250 bits fails. The initial and final design of the cutting bit can be seen in Fig. 4 and the largest principal stress for both designs can be seen in Fig. 5.

It is seen from Fig. 5 that the largest principal stress has been reduced significantly as expected. However, if the objective of the shape optimization is to reduce the largest principal stress, the final shape becomes slightly different. This is due to the volume dependence involved in the expression for probability of failure, see (1). A stress minimized design tends to have large volumes with uniform maximum stress



$P_f = 4.7\%$: 1 out of 21 fails



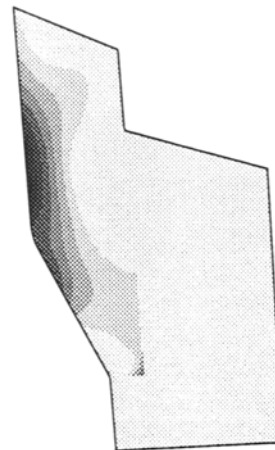
$P_f = 0.0014\%$: 1 out of 7250 fails

Fig. 4. Initial and final design of cutting bit from a circular saw blade

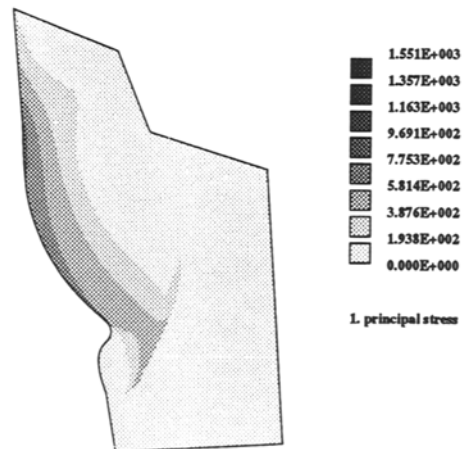
but this is usually not the best design of a brittle material as a larger volume has a larger probability of containing big flaws than a smaller volume of the structure. This tendency of difference between stress minimized designs and failure minimized designs is even more pronounced in cases where the second principal stress is positive and nearly equal to the largest principal stress, cf. the definition of the equivalent stress in Table 1. In such situations there might be a big difference in optimum design between using the probability of failure or the largest principal stress as objective. This important fact has been demonstrated by Rasmussen and Lund (1997) in the case of designing a turbine disk of ceramic material.

7 Conclusions

In this paper an application of shape optimization has been discussed. The objective has been to take into account the



Max. $\sigma_1 = 1551$ MPa



Max. $\sigma_1 = 858$ MPa

Fig. 5. First principal stress in initial and final design of cutting bit

probability of failure of components made of brittle materials in the design process. The analysis of probability of failure is based on a generally accepted two-parameter model using Weibull's probabilistic treatment of brittle strength. Expressions for design sensitivities have been derived analytically and it has been shown how it can be implemented in a finite element based analysis system. A test specimen example is used for numerical verification of the facilities for analysis and design sensitivity analysis. Finally, an industrial example illustrates the effectiveness of designing mechanical components made of brittle materials by using Weibull probabilistic methods combined with finite element based shape optimization and mathematical programming.

References

Andreasen, J. 1993: Statistics of brittle failure in multiaxial stress states. *J. Amer. Ceramic Soc.* **76**, 2933-2935

- Andreasen, J. 1994: Reliability-based design of ceramics. *Materials & Design* 15, 3-13
- Evans, A. 1978: A general approach to the statistical analysis of multiaxial fracture. *J. Amer. Ceramic Soc.* 61, 302-308
- Koski, J.; Silvennoinen, R. 1990: Multicriteria design of ceramic components. In: Eschenauer, H.A.; Koski, J.; Osyczka, A. (eds.) *Multicriteria design optimization*, pp. 447-463. Berlin, Heidelberg, New York: Springer
- Lund, E. 1994: *Finite element based design sensitivity analysis and optimization*. Ph.D. Thesis, Aalborg University, Denmark
- Lund, E.; Olhoff, N. 1994: Shape design sensitivity analysis of eigenvalues using "exact" numerical differentiation of finite element matrices. *Struct. Optim.* 8, 52-59
- McLean, A.F.; Hartsock, D.L. 1989: Design with structural ceramics. In: Wachtman, J.B. (ed.) *Structural mechanics*, pp. 22-97. London: Academic Press
- Olhoff, N.; Rasmussen, J.; Lund, E. 1993: A method of "exact" numerical differentiation for error elimination in finite element based semi-analytical shape sensitivity analysis. *Mech. Struct. & Mach.* 21, 1-66,
- Rasmussen, J.; Lund, E. 1997: The issue of generality in design optimization systems. *Eng. Opt.* (to appear)
- Rasmussen, J.; Lund, E.; Olhoff, N. 1993: Integration of parametric modeling and structural analysis for optimum design. In: Gilmore, B.J.; Hoeltzel, D.A.; Azarm, S.; Eschenauer, H.A. (eds.) *Advances in design automation*, pp. 637-648. New York: The American Society of Mechanical Engineers
- Vardar, Ö.; Finnie, I. 1975: An analysis of the Brazilian disk fracture test using the Weibull probabilistic treatment of brittle strength. *Int. J. Fracture* 11, 495-508
- Weibull, W. 1939: A statistical theory of the strength of materials. *Ingeniörs Vetenskaps Akademien, Handlingar* 151, 5-45

Received April 27, 1997

Revised manuscript received Oct. 20, 1997